npj | climate and atmospheric science

www.nature.com/npjclimatsci

ARTICLE OPEN

Check for updates

# Evaluation of tornadic environments and their trends and projected changes in Japan

Sho Kawazoe[1]✉, Masaru Inatsu[1], Mikiko Fujita[2], Shiori Sugimoto[2], Yasuko Okada[2] and Shingo Watanabe[2]

Tornadoes are responsible for several high-impact weather disasters in Japan. However, little is known about how these events have changed over the last several decades or how they may change in future climates. This study examines environmental conditions associated with tornados in Japan using pseudo-soundings from the high-resolution fifth-generation ECMWF reanalysis. We first determine appropriate discriminators of F2+ tornadoes using thermodynamic (convective available potential energy, convective inhibition, lifting condensation level, and the K-index), kinematic (bulk wind difference and storm-relative helicity), and multivariate tornado parameters (energy helicity index, K-helicity index, and the significant tornado parameter), and confirm that F2+ tornadoes occur in environments with higher instability and helicity, but are better distinguished using multivariate parameters. Recent trends indicate that F2+ environments have increased significantly in some regions over the last four decades. We also examined future changes for each parameter using a large ensemble 2-K warming experiment. Robust increases in strong tornado environments are depicted in many regions in Japan, particularly on the Sea of Japan side and the Kanto region. This indicates that despite projected decreases in bulk wind difference and higher convective inhibition, significant increases in atmospheric instability compensate, leading to more days with F2+ tornado potential.

*npj Climate and Atmospheric Science* (2023)6:199 ; https://doi.org/10.1038/s41612-023-00524-x

## INTRODUCTION

As the scientific evidence linking anthropogenic warming to increases in extreme weather events mounts, there is considerable interest in how severe convective storms may respond. The most violent types of convective storms are those capable of producing tornadoes, which garner particular attention due to their destructive and unpredictable nature. However, many challenges exist when examining tornadic responses to climate change. Aside from the many knowledge gaps on tornadoes, they also include the inhomogeneity in reporting and damage assessments, spatially and temporally sparse radiosonde data, and incomplete or limited archives of historical events. These problems are further exacerbated when examined globally due to the lack of uniformity in the standards of tornado reporting between countries. For Japan, in addition to the lack of dense observational stations, sounding reports are only available (aside from a few sporadic reports) at 0900 and 2100 Japan Standard Time (JST; 0000 and 1200 UTC). This potentially limits the number of events commonly considered environments associated with tornadoes (i.e., within 3 h), typically occurring between 1100 JST and 1800 JST (Supplementary Fig. 1a).

To alleviate the problems posed by non-homogeneous and scarce radiosonde data, pseudo-proximity (grid point) soundings are commonly used in their place. Gridded soundings can provide better insight into severe convective environments, including tornadoes, as they offer higher spatiotemporal resolution than observations. While the majority of studies utilizing pseudo-proximity soundings for convective environments are focused in the United States[1–5], the quantitative understanding obtained from those studies has led to their use, primarily by global reanalysis, in examining tornadic and other severe convective environments throughout the world[6–11].

As we develop a deeper understanding of severe convective environments, studies on their climatology, recent trends, and anticipated changes in response to a warming climate have been performed. In terms of recent trends in severe convective environments, the general understanding is that as the climate has warmed, there is greater potential for atmospheric instability and convective potential. By the same notion, deep layer vertical wind shear, an important component for storm organization, has weakened in the mid-latitudes due to decreased meridional temperature gradient[12]. However, changes vary significantly both seasonally and regionally due to complex differences in regional and atmospheric characteristics[13–15], so it is important to examine how severe weather events, in the case of this study, tornadic environments, change on a regional level. Studies examining future changes commonly use relatively coarse resolution models, acknowledging that while convective thunderstorms may not be explicitly resolved, which encounter limitations due to high computational demand, an implicit understanding of future changes in convective environments can be achieved while allowing us to evaluate their uncertainties[16–21]. To date, only Muramatsu et al. [22] have investigated future changes in tornado environments over Japan. However, their results were based only on one model ensemble for the end-of-century climate, and indices for tornado environments were determined based on tornadoes in the United States at coarser time increments, which may not represent tornadoes over Japan

This study aims to expand upon previous studies to provide a comprehensive perspective of tornadic events in Japan using environmental proxies. We first examine the ability of several commonly used convective parameters that govern severe weather development through reanalysis datasets. These include common measures for strong convective potential [convective available potential energy (CAPE), convective inhibition (CIN), and the K-index (KI)] and the bulk wind difference (BWD). In addition, the lifting condensation level (LCL) and storm-relative helicity (SRH), which represents low-level moisture and updraft rotation

[1]Hokkaido University, Sapporo, Japan. [2]Japan Agency for Marine-Earth Science and Technology, Yokohama, Japan. ✉email: kawazoe@sci.hokudai.ac.jp

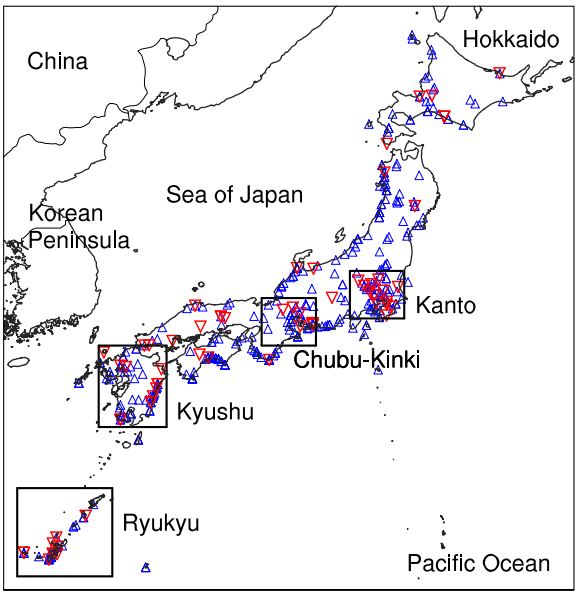


**Fig. 1 Tornado reports from 1979 – 2021 used in this study.** Red triangles indicate F2+ tornadoes and blue triangles indicate F0 and F1 tornadoes. Black boxes indicate domains used for trend analysis.

indicative of tornadic potential, are also investigated. Multivariate parameters that combine these indices [Energy Helicity Index (EHI), K-Helicity index (KHI), and the Significant Tornado Parameter (STP)] are then examined for a clearer understanding of environments that distinguish between weak and significant tornadoes. Lastly, we evaluate how their frequency has and may change in the near future using reanalysis and a high-resolution large ensemble regional climate experiment.

## RESULTS

### Identifying tornadic environments and their recent trends

Based on 469 tornadic events (67 F2+ on the Fujita scale, 215 F1, and 187 F0; Fig. 1), Fig. 2 shows boxplots of each parameter as a function of tornado intensity using the ERA5$_m$. Consistent with previous studies, stronger tornadoes exhibit higher instability (CAPE and KI), low-level moisture (LCL), and stronger SRH. The slightly stronger CIN for F2+ tornadoes may indicate that stronger buoyant updrafts can overcome moderate levels of CIN or assist in capping weak convective initiation until environments are more favorable or built up for intense convection. The BWD does not differ significantly between intensities, consistent with Thompson et al. [1] and others, indicating that other environmental contributions distinguish tornadic intensity once BWD is sufficiently strong for convective development. The EHI, KHI, and STP indices discriminate between tornadic intensities reasonably well, though

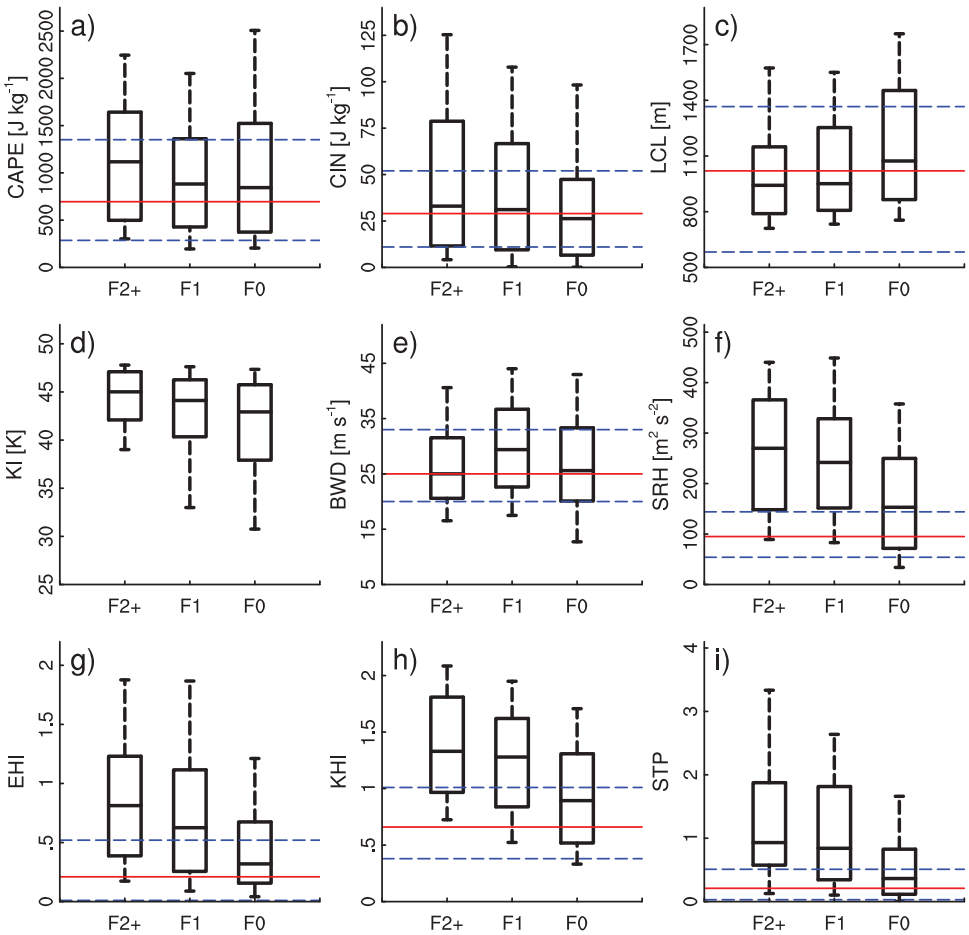


**Fig. 2 Box and whisker plots from pseudo-proximity soundings from the ERA5$_m$. a** CAPE, (**b**) CIN, (**c**) LCL, (**d**) KI, (**e**) BWD, (**f**) SRH, (**g**) EHI, (**h**) KHI, and (**i**) STP in the proximity of tornadoes in Fig. 1, separated by the Fujita scale rating. The boxes extend to the 25th and 75th percentiles, and the horizontal line within the box represents the median. Whiskers represent the 10th and 90th percentiles. The dotted blue line represents the 25th and 75th percentiles, and the solid red line represents the median for F2+ tornadoes from the ERA5$_p$.

there are considerable overlaps in distribution. While there are limitations to these indices, as evidenced by the overlaps, we determine that values of 0.7 (EHI), 1.3 (KHI), and 1 (STP) are reasonable indicators of F2+ environments for Japan using the $ERA5_m$. We note that median EHI and STP values are roughly two to three times lower than F2+ environments in the United States[1,3]. This is due to higher CAPE environments over the United States, where median values for F2+ in Thompson et al. [1] are more than twice what is shown in Fig. 2. This also likely explains the lack of recorded F4+ tornadoes over Japan. Additionally, thresholds for EHI, KHI, and STP using the $ERA5_p$ are 0.5, 1, and 0.5, respectively (Fig. 2 and Supplementary Fig. 2). This is needed for our climate change analysis, as the simulations for this study are also on pressure-level coordinates.

**Table 1.** Forty-three year trend statistics (per decade) for each parameter.

| | Kanto | Chubu-Kinki | Kyushu | Ryukyu |
|---|---|---|---|---|
| CAPE | 94.84** | 69.87** | 78.59* | 37.91 |
| CIN | 5.63** | 2.87** | 1.72** | 1.00** |
| LCL | 18.05** | 17.35** | 12.08* | 85.70* |
| KI | 0.40** | 0.27** | 0.27** | 0.39** |
| BWD | −0.29 | −0.20 | −0.17 | −0.18 |
| SRH | 0.17 | −0.33 | −0.18 | −0.14 |
| EHI | 1.96** | 1.23 | 3.29* | 8.20* |
| KHI | 0.54 | 0.98 | 0.98 | 0.50 |
| STP | 0.42* | 0.48 | 1.15 | 1.94 |

Regions in Fig. 1. Theil-Sen slope values are computed at percentiles used in Fig. 4. Single asterisk indicates statistically significant trends at $p$ value < 0.05 and double asterisk at $p$ value < 0.01, using the non-parametric statistical Mann–Kendall test.

Long-term trends (1979–2021) for F2+ environments in several regions with a high frequency of F2+ events (Fig. 1) are shown in Table 1 and Fig. 3. As expected, areas further south exhibit more hours with F2+ environments, mainly due to the influence of higher atmospheric instability (CAPE and KI). Long-term trends are mixed between regions and tornadic indices. Significant trends ($p$-value < 0.05) are seen for EHI and STP in Kanto and EHI in Kyushu and Ryukyu. The KHI exhibits the lowest interannual variability magnitude, likely culminating in a muted trend signal. The overall increasing trends can largely be attributed to the increasing trends in CAPE and KI, as BWD and SRH show insignificant trends (Table 1). CIN and LCL have shown a gradual but significant increase in all regions due to decreasing low-level relative humidity[23], which is unfavorable for tornadic environments. It is noted that in addition to increasing trends in instability, there are significantly increasing trends in tropical cyclone frequency (Supplementary Fig. 3), which accounts for roughly 20% of all tornado events in Japan[9], which may have influenced some long-term trends of F2+ environments, particularly in Ryukyu, where significantly increasing trends in EHI is not in supported by trends in the individual parameters used to compute EHI. The lone region with no significant trends in tornado parameters is the Chubu-Kinki region, despite significant

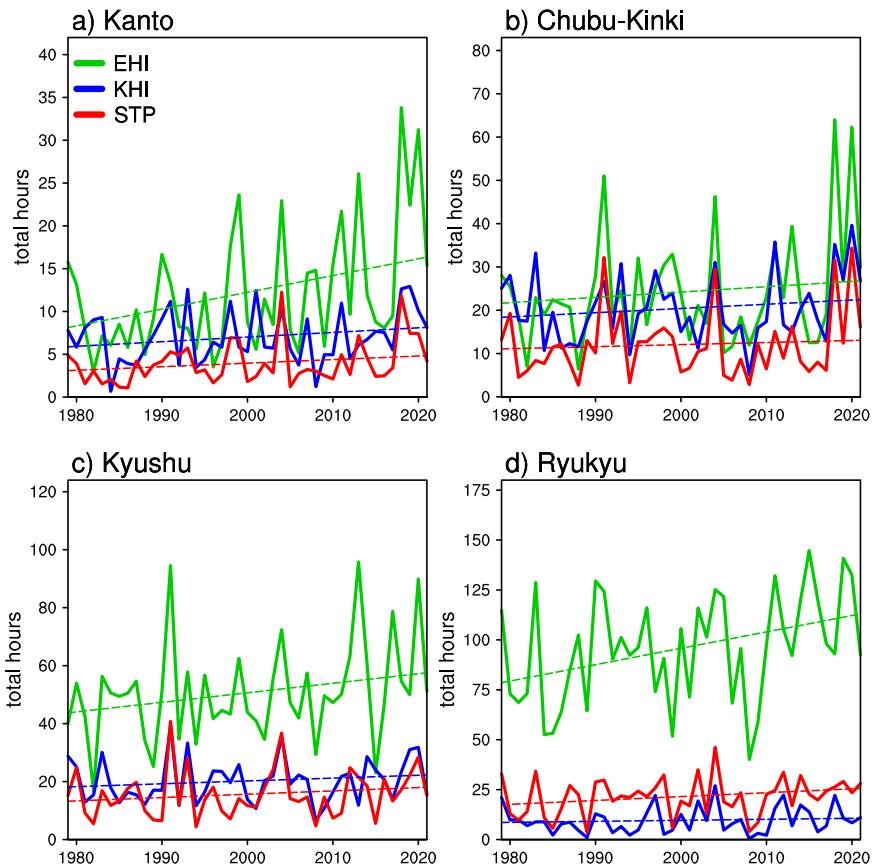


**Fig. 3 Forty-three year (1979–2021) timeseries of F2+ tornado environments.** Annual 3-h frequency using the $ERA5_m$ for EHI > 0.7, KHI > 1.3, and STP > 1 over the (**a**) Kanto, (**b**) Chubu-Kinki, (**c**) Kyushu, and (**d**) Ryukyu regions shown in Fig. 1. Dashed lines represent the 43-year trend using the Theil-Sen slope estimate.

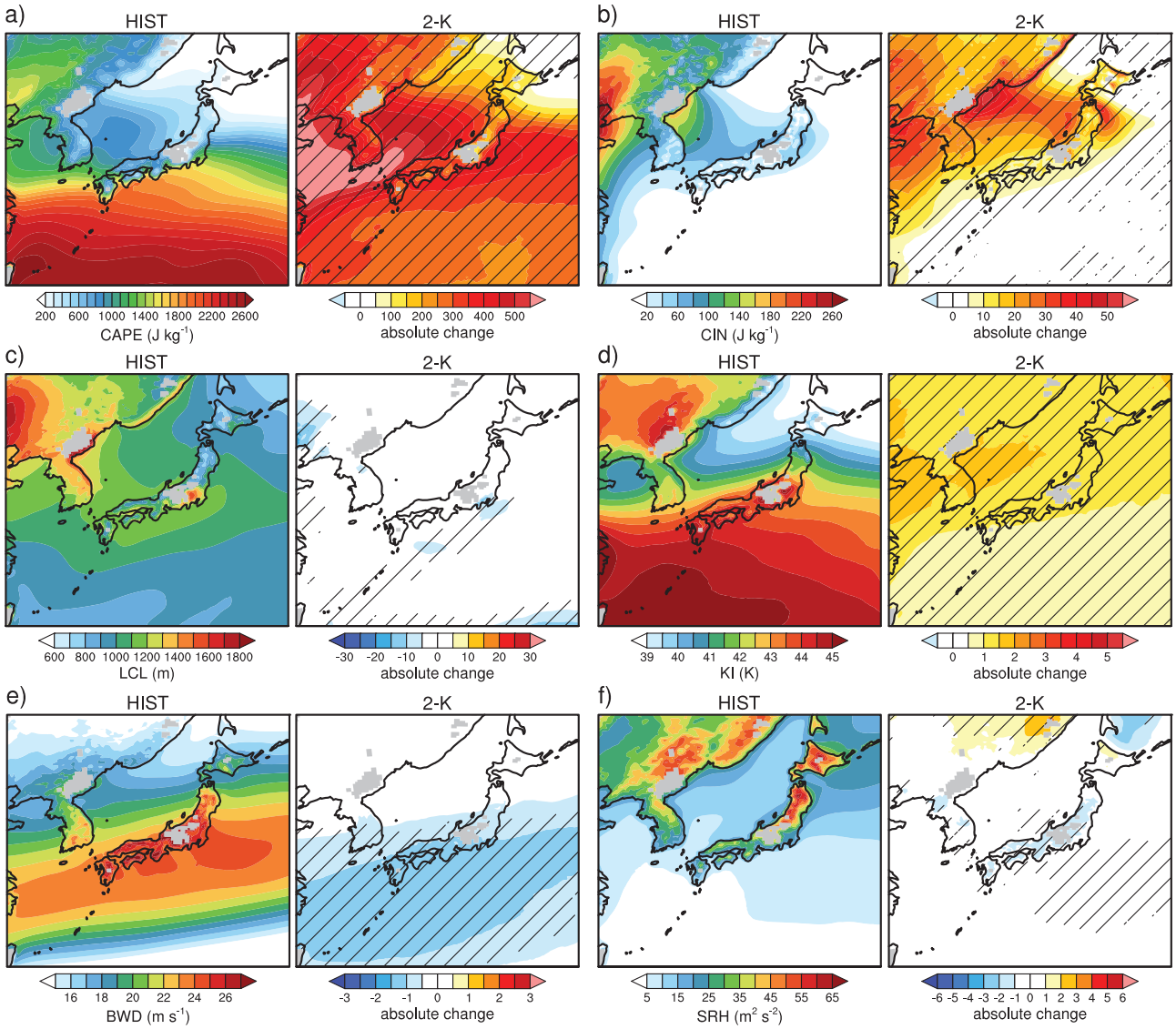


**Fig. 4 Spatial distribution of convective parameters and their future changes.** (left) HIST ensemble mean, and (right) absolute change between the 2-K ensemble mean and HIST ensemble mean for (**a**) 95th percentile CAPE, (**b**) 95th percentile CIN, (**c**) median LCL, (**d**) 95th percentile KI, (**e**) median BWD, and (**f**) median SRH. Hatching indicates agreement in the response across all 2-K members.

trends in CAPE and KI. Note, however, that the highest frequency of tornado environments has occurred in recent years.

## Model validation and future changes in tornadic environments

The HIST is compared with the ERA5$_p$ for thermodynamic and kinematic parameters, as the d4PDF provides model output at pressure levels. The HIST (Fig. 4) reproduces the spatial distribution of the ERA5$_p$ (Supplementary Fig. 3). Prominent features include stronger atmospheric instability (CAPE, KI) in the southern portion of our domain due to high lower tropospheric moisture. Higher values are also depicted on the Pacific Ocean side compared to the Sea of Japan side, likely for the same reason. For CIN, high values are seen over China and portions of the Korean Peninsula, typically generated from warming at high elevations and subsidence of dry air from continental westerlies. Similar characteristics to CIN are also seen for LCL. Differences between HIST and ERA5$_p$ CIN are most pronounced over water east of the landmass, which may indicate that warm low-level airmass off land that commonly produce high CIN over water are weaker in simulations. BWD follows the climatological location of the mid-latitude jet, which is highest near central Japan. Lastly, SRH is greater at higher latitudes and over land. This region frequently experiences the passage of extratropical cyclones[24,25], which can produce strong near-surface winds. The resulting low-level shear induced by surface friction is likely depicted here[11].

For +2-K changes, we focus on areas where all ensembles agree on the sign of the change (Fig. 4). Atmospheric instability parameters exhibit an increase across the analysis domain, primarily due to a projected increase in low-level specific humidity (not shown). For CIN, there is an increase over Japan and areas to the west. The spatial distribution is comparable to Chen et al. [26], who examined end-of-century changes to CIN using the CCSM4, which is one of the ΔSST patterns for d4PDF. LCL exhibits minimal change in 2-K, with only the Kanto region and parts of China showing slightly lowering LCL heights consistent across ΔSST patterns. This lowering of LCL is due to a subtle increase in projected relative humidity (not shown), which, interestingly, differs from the observed trends. However, we note that while

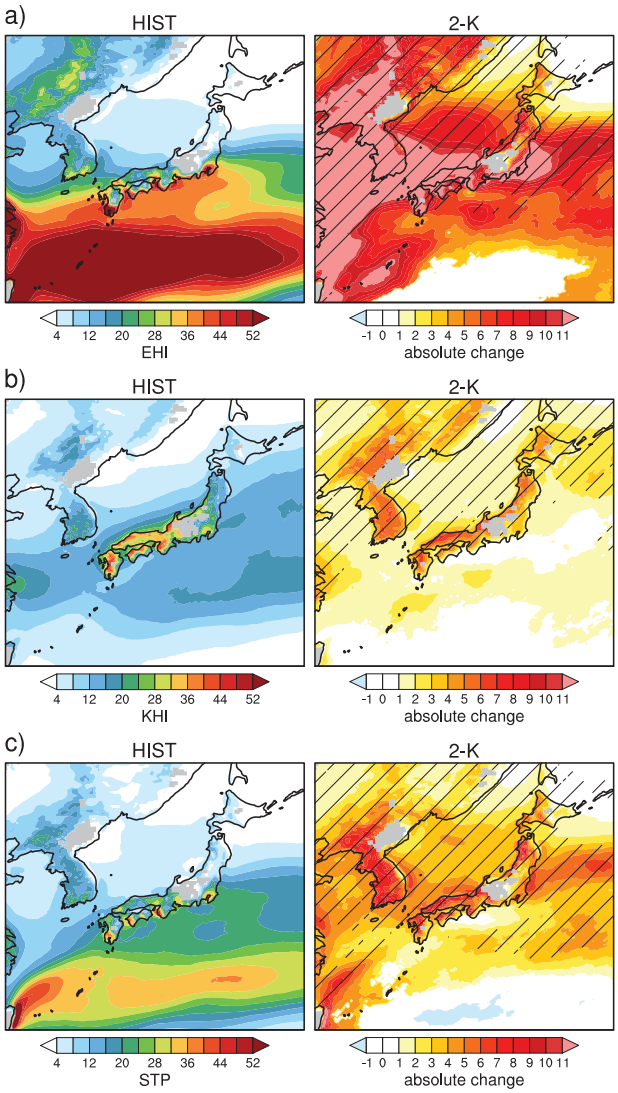


**Fig. 5 Spatial distribution of F2+ tornado environment frequency and their future changes. a** EHI > 0.5, (**b**) KHI > 1, and (**c**) STP > 0.5.

low-level relative humidity from the ERA5 also showed decreasing trends throughout much of Japan from 1979–2010, the HIST ensemble showed no significant trend (not shown), which may explain the differences between observed and climate simulations in some areas. For BWD, decreases in meridional temperature gradients due to warming temperatures to the north act to weaken mid-latitude vertical shear, as reported in previous studies[21]. Lastly, small negative differences in SRH are depicted over Japan, which may be attributed to a projected delay in the Baiu front onset[27,28] or a decrease in cyclone passage in future climates[25], acting to reduce low-level wind shear.

The spatial distribution of EHI, KHI, and STP frequencies is shown in Fig. 5. A higher frequency of F2+ tornado environments is depicted in the southern portion of mainland Japan, such as Kanto and Kyushu, consistent with high CAPE and KI. High EHI and STP values are exhibited near the coast, while the KHI is distributed uniformly over land. This is due to the sensitivity of surface elevation and the lifted parcel in computing CAPE compared to KI, which uses specific pressure levels. Over the Ryukyu region, very few F2+ events are depicted in KHI due to low SRH values. The +2-K responses are mostly consistent between tornado parameters in depicting northern Japan to have more hours with F2+ environments, with more pronounced changes in June–August (Supplementary Fig. 5). This also signals that increases in F2+ environments occur primarily during the first half of the peak observed tornado season (Supplementary Fig. 1b) and less so in the second half (September–November). Greater changes are exhibited on the Sea of Japan side, synonymous with areas with larger changes in atmospheric instability compared to the Pacific Ocean side. The clear exception is in the Kanto region for EHI, which also sees high magnitude change in CAPE comparable to the Sea of Japan side. These features are muted for STP because of the introduction of LCL and BWD, which are projected to decrease slightly in +2-K. In contrast, the KHI exhibits smaller changes compared to EHI and STP. This is due to the difference in projected change between CAPE and KI, as CAPE in some areas can double from HIST, while KI increases only by 1–2 K. Lastly, the spatial distribution of EHI, KHI, and STP separated by ΔSST patterns are shown in Supplementary Fig. 6, confirming the +2-K changes over Japan are in agreement that more frequent F2+ environments should be expected, regardless of the tornado parameter. The clear difference to the +2 K changes is near the Ryukyu islands, where the future ensemble does not show agreement across members in any tornado parameter (Fig. 5), especially in SON (Supplementary Fig. 5) and across ΔSST patterns (Supplementary Fig. 6). It is possible that projected decreases in tropical cyclone activity in future climates in this region, as highlighted in many studies[25,29,30], and differences in the magnitude changes, may have contributed to the uncertainty in this region's projected changes.

## DISCUSSION

In this study, we investigate the climatology of F2+ tornadic environments in Japan, how they have changed over the last few decades, and how they may continue to change in response to global warming. The development of the high spatial and temporal resolution ERA5 reanalysis allows for a better understanding of tornadic events in Japan, which has yet to be possible with observational soundings or coarser resolution reanalysis. From this, we were able to confirm what has been concluded in many studies, which is that F2+ tornadoes can be discriminated from weak tornadoes based on commonly used thermodynamic and kinematic parameters, and much better using multivariate parameters.

Trends using multivariate parameters suggest several regions with statistically significant increasing trends in F2+ environments. While the long-term increasing trend can partly be attributed to long-term increases in atmospheric instability, which is strongly related to regional warming trends, it does not fully explain these recent features. It would be interesting to monitor these environmental characteristics to determine whether they can be attributed to climate change or are more likely a response to internal climate variability. Additionally, further insight may be gained by using the recently extended ERA5, which now dates to 1940 but was not openly available at the time of this study. Compared to HIST, the +2-K climate shows much of Japan with increasing F2+ environments. Northern regions of Japan are expected to see nearly a doubling of F2+ environments based on EHI, KHI, and STP (Fig. 5). Eastern and southern Japan near Kanto, Chubu-Kinki, and Kyushu regions also showed increases in most indices. However, we note that some ΔSST patterns showed similar or even slight decreases in frequency. The primary driver is increased atmospheric instability, which is closely linked to increases in near-surface temperatures.

The F2+ tornado environments are projected to increase in some of Japan's most densely populated regions, some of which may already be observed, as evidenced by trends in atmospheric instability and some multivariate tornado parameters. Therefore, the general public should be increasingly conscious of the dangers of tornadoes, and appropriate preparation should be undertaken to mitigate their societal impacts. For the forecast and research community, tornado-related indices should be

continually re-examined and refined as we develop a more robust understanding of tornadogenesis through enhancements in numerical simulations, observational and reanalysis datasets, and larger tornado observation sample sizes.

In future studies, it is desirable to evaluate climate models at convective permitting (<4 km) resolutions, preferably with model-level vertical coordinates, as the $ERA5_m$ exhibits clear advantages compared to $ERA5_p$ in the representing convective environments. Many have shown the benefits of convective permitting models by simulating convective thunderstorms explicitly or for greater spatial and temporal representation of tornado environments that implicit methods may fail to capture, particularly when determining if adequate triggering mechanisms exist to initial convection, justifying the heavy computation burden necessary to perform such simulations[31–35]. Additionally, the representation of F2+ environments is highly sensitive to the indices applied, as our study suggests. Muramatsu et al. [22] also examined changes in F2+ tornadic environments using a threshold of CAPE ≥ 500 J kg$^{-1}$ and surface to 3 km SRH ≥ 150 m$^2$ s$^{-2}$, which was determined for tornadoes in the U.S., using 6-h reanalysis data. In their 1993–2003 JJA model results, F2+ frequency near Kanto is ~4.5, and ~11 for Kyushu (approximated from Fig. 7 in Muramatsu et al. [22]), all lower than our JJA results using $ERA5_p$ (not shown). It is also important to note that regardless of which tornado indices are used, they serve as guidance for operational forecasters to determine the potential for tornadoes. As such, there are likely a decent number of missed forecasts and even more false alarms. Finally, as Tochimoto[36] comprehensively reviews, tornadoes can develop under various synoptic and mesoscale environments. Therefore, further studies, preferably with much larger sample sizes, should be performed in the future. All these factors contribute to recognizing that future increases in environments favorable for strong tornadoes should not be assumed as more tornadoes are on the ground. Continued research is required in many aspects of tornado environments.

## METHODS

CAPE and KI quantify the potential for strong convective thunderstorm development. CIN suppresses moist convection development by producing negative buoyant energy in the lower troposphere. LCL heights signify abundant low-level moisture and the cloud base, which can be useful in distinguishing between violent and non-violent tornados[37,38]. BWD promotes convective organization, and SRH represents the potential of updraft rotation of convective storms. The formulas for each parameter are detailed in Supplementary Table 1.

Previous studies have shown that the multivariate relationship of several thermodynamic and kinematic indices better distinguishes tornado events from non-tornadic convection and tornado intensity. Therefore, we used three co-variate tornado parameters to examine environments favorable for F2+ tornadoes: the EHI[2]:

$$\mathrm{EHI} = \frac{\mathrm{CAPE} \times \mathrm{SRH}}{160,000} \tag{1}$$

the slightly modified KHI[39]:

$$\mathrm{KHI} = \frac{\mathrm{KI}^2 \times \sqrt{\mathrm{SRH}}}{20,000} \tag{2}$$

And the STP[1]:

$$\mathrm{STP} = \frac{\mathrm{CAPE}}{1000\,\mathrm{J\,kg^{-1}}} \times \frac{\mathrm{SRH}}{100\,\mathrm{m^2 s^{-2}}} \times \frac{\mathrm{BWD}}{20\,\mathrm{m\,s^{-1}}} \times \frac{2000\,\mathrm{m} - \mathrm{LCL}}{1500\,\mathrm{m}} \tag{3}$$

For each parameter, an environment where CIN > 125 J kg$^{-1}$ (approximately the 90th percentile of F2+ tornadoes in Fig. 2) is omitted.

### Tornado database

Damaging wind gust events from 1961 onward are archived by the Japan Meteorological Agency's tornadoes and severe winds database. The dataset provides the type of event (tornado, downburst, gust front, funnel cloud, dust devil), intensity, time, location, and prevailing meteorological conditions such as a passage of a cold front or a presence of an upper-level pressure trough. For this study, we focus on tornadic events between 1979 and 2021. Any tornadic reported over water or without intensity, location, or occurrence time is omitted. To avoid duplicate reports, we assume all reports that occurred within 30 min and 0.3° to be from the same parent thunderstorm, and the highest intensity reports are used. Several changes have been implemented since the start of this archive, most notably to the rating system to estimate tornado intensities. The Japanese Enhanced Fujita scale was implemented in April 2016 to replace the Fujita scale based on differences in damage assessment between Japan and the United States. For simplicity, however, we assume these changes to be negligible.

### Reanalysis

Pseudo-proximity sounding utilizes the European Centre for Medium-Range Weather Forecasts high-resolution reanalysis (ERA5[40]). At the time of this study, the ERA5 provides the highest spatial and temporal resolution among reanalysis datasets available (~31 km grid spacing). For three-dimensional computations, we use hourly outputs at 29 pressure levels from 1000 to 100 hPa for $ERA5_p$ and 78 hybrid/sigma model levels from near-surface to ~100 hPa from the $ERA5_m$. The $ERA5_m$ dataset has been shown to better reproduce convective and kinematic parameters from radiosondes observations than coarser resolution reanalysis[41]. Similar conclusions are seen when we compare $ERA5_m$ soundings to coarser resolution reanalyzes such as the Japanese 55-year reanalysis (JRA-55[42]) or pressure level data from the $ERA5_p$[43] (Supplementary Table 2 and Supplementary Fig. 7). This is particularly true for parameters requiring high vertical resolution at lower levels (CAPE, CIN, SRH). These results demonstrate that higher horizontal and vertical resolution in the $ERA5_m$ is better suited for convective environment evaluation.

To evaluate tornadic environments, we extract the maximum values for each parameter from the closest hourly reanalysis soundings and within a 0.75° grid box for each tornado report.

### Ensemble climate simulations

Dynamically downscaled regional simulation from the database for Policy Decision-Making for Future Climate Change (d4PDF[44,45]) large ensemble dataset is used for historical and future climate simulations. Downscaling experiments from a 60-km atmospheric general circulation (AGCM) to 20 km were performed using the non-hydrostatic regional climate model (NHRCM[46]). Each ensemble simulation contains 60 years of historical (1951–2010; HIST) and a 2-K warming scenario. Fifty HIST AGCM ensemble members were created using different initial conditions, and small sea surface temperature (SST) perturbations were downscaled using the NHRCM. The 2-K scenario represents a climate that is 2-K warmer relative to pre-industrial levels, corresponding to a climate around 2040 under the Coupled Model Intercomparison Project phase 5 Representative Concentration Pathway 8.5 scenario. Fifty-four ensembles were created by adding SST warming patterns (ΔSST) from six CMIP5 simulations. Due to computational limitations in storing and computing environmental parameters with three-dimensional data, we examine 320 years for HIST (10 members × years 1979–2010) and 1800 years for 2-K (5 members × 6 ΔSST × 60 years). We used 6-h output at the same 29 pressure levels as the reanalysis.

## DATA AVAILABILITY

Radiosonde data was downloaded from the University of Wyoming sounding database (http://weather.uwyo.edu/upperair/sounding.html). Tornado reports are provided by JMA's database of tornadoes and severe winds, available at (https://www.data.jma.go.jp/obd/stats/data/bosai/tornado/). The ERA5 hourly data was downloaded from the Copernicus Climate Change Service (https://cds.climate.copernicus.eu/). The JRA-55 dataset was downloaded from the Research Data Archive at the National Center for Atmospheric Research, Computational, and Information Systems Laboratory, available at (https://rda.ucar.edu/). The d4PDF datasets were downloaded from the Data Integration and Analysis System Program (DIAS; https://diasjp.net/en/).

## CODE AVAILABILITY

The codes used for the analysis are available upon reasonable request from the corresponding author.

Received: 31 March 2023; Accepted: 11 November 2023;
Published online: 28 November 2023

## REFERENCES

1. Thompson, R. L., Edwards, R., Hart, J. A., Elmore, K. L. & Markowski, P. Close proximity soundings within supercell environments obtained from the Rapid Update Cycle. *Weather Forecast.* **18**, 1243–1261 (2003).
2. Rasmussen, E. N. Refined supercell and tornado forecast parameters. *Weather Forecast.* **18**, 530–535 (2003).
3. Grams, J. S. et al. A climatology and comparison of parameters for significant tornado events in the United States. *Weather Forecast.* **27**, 106–123 (2012).
4. Gensini, V. A. & Ashley, W. S. Climatology of potentially severe convective environments from the North American Regional Reanalysis. *E J. Sev. Storms Meteorol.* **6**, 1–40 (2011).
5. Gensini, V. A., Converse, C., Ashley, W. S. & Taszarek, M. Machine learning classification of significant tornadoes and hail in the United States using ERA5 proximity soundings. *Weather Forecast.* **36**, 2143–2160 (2019).
6. Brooks, H. E., Lee, J. W. & Craven, J. P. The spatial distribution of severe thunderstorm and tornado environments from global reanalysis data. *Atmos. Res.* **67-68**, 73–94 (2003).
7. Allen, J. T. & Karoly, D. J. A climatology of Australian severe thunderstorm environments 1979–2011: inter-annual variability and ENSO influence. *Int. J. Climatol.* **34**, 81–97 (2014).
8. Tippett, M. K., Allen, J. T., Gensini, V. A. & Brooks, H. E. Climate and hazardous convective weather. *Curr. Change Rep.* **1**, 60–73 (2015).
9. Sueki, K. & Niino, H. Toward better assessment of tornado potential in typhoons: Significance of considering entrainment effects for CAPE. *Geophys. Res. Lett.* **43**, 12597–12604 (2016).
10. Taszarek, M., Brooks, H. E., Czernecki, B., Szuster, P. & Fortuniak, K. Climatological aspects of convective parameters over Europe: a comparison of ERA-Interim and sounding data. *J. Clim.* **31**, 4281–4308 (2018).
11. Tochimoto, E. & Niino, H. Structure and environment of tornado-spawning extratropical cyclones around Japan. *J. Meteorol. Soc. Jpn.* **96**, 355–380 (2018).
12. Diffenbaugh, N. S., Trapp, R. J. & Brooks, H. Does global warming influence tornado activity? *EOS* **89**, 53 (2011).
13. Zhang, Q., Ni, X. & Zhang, F. Decreasing trend in severe weather occurrence over China during the past 50 years. *Sci. Rep.* **7**, 42310 (2017).
14. Gensini, V. A. & Brooks, H. E. Spatial trends in United States tornado frequency. *npj Clim. Atmos. Sci.* **1**, 38 (2018).
15. Taszarek, M., Allen, J. T., Marchio, M. & Brooks, H. E. Global climatology and trends in convective environments from ERA5 and rawinsonde data. *npj Clim. Atmos. Sci.* **4**, 35 (2021).
16. Trapp, R. J. et al. Changes in severe thunderstorm environment frequency during the 21st century caused by anthropogenically enhanced global radiative forcing. *Proc. Natl Acad. Sci.* **104**, 19719–19723 (2007).
17. Gensini, V. A., Ramseyer, C. & Mote, T. L. Future convective environments using NARCCAP. *Int. J. Climatol.* **34**, 1699–1705 (2013).
18. Takemi, T. Projected regional-scale changes in atmospheric stability condition for the development of summertime convective precipitation in the Tokyo metropolitan area under global warming. *Hydrol. Res. Lett.* **6**, 17–22 (2012).
19. Diffenbaugh, N. S., Scherer, M. & Trapp, R. J. Robust increases in severe thunderstorm environments in response to greenhouse forcing. *Proc. Natl Acad. Sci.* **110**, 16361–16366 (2013).
20. Púčik, T. et al. Future changes in European severe convection environments in a regional climate model ensemble. *J. Clim.* **30**, 6771–6794 (2017).
21. Lepore, C., Abernathey, R., Henderson, N., Allen, J. T. & Tippett, M. K. Future global convective environments in CMIP6 models. *Earth's Future* **9**, e2021EF002277 (2021).
22. Muramatsu, T., Kato, T., Nakazato, M., Endo, H. & Kitoh, A. Future changes of tornadogensis-favorable environmental conditions in Japan estimated by a 20-km-mesh atmospheric general circulation model. *J. Meteorol. Soc. Jpn.* **94A**, 105–120 (2016).
23. Shibata, K. & Sai, A. Long–term trends and variations in surface humidity and temperature in the Japanese archipelago over 100 years from 1880s. *J. Meteorol. Soc. Jpn.* **99**, 403–422 (2021).
24. Lee, J. et al. Extratropical cyclones over East Asia: climatology, seasonal cycle, and long-term trend. *Clim. Dyn.* **54**, 1131–1144 (2020).
25. Kawazoe, S., Inatsu, M., Yamada, T. J. & Hoshino, T. Future changes in tropical and extratropical cyclones affecting Hokkaido and their related precipitation based on large-ensemble climate simulations. *J. Appl. Meteorol. Climatol.* **62**, 341–359 (2023).
26. Chen, J., Dai, A., Zhang, Y. & Rasmussen, K. L. Changes in convective available potential energy and convective inhibition under global warming. *J. Clim.* **33**, 2025–2050 (2020).
27. Kusunoki, S., Mizuta, R. & Matsueda, M. Future changes in the East Asian rain band projected by atmospheric models with 20-km and 60-km grid size. *Clim. Dyn.* **37**, 2481–2493 (2011).
28. Okada, S., Takemi, T., Ishikawa, H., Kusunoki, S. & Mizuta, R. Future changes in atmospheric conditions for the seasonal evolution of the Baiu as revealed from projected AGCM experiments. *J. Meteorol. Soc. Jpn.* **95**, 239–260 (2017).
29. Yoshida, K., Sugi, M., Mizuta, R., Murakami, H. & Ishii, M. Future changes in tropical cyclone activity in high-resolution large-ensemble simulations. *Geophys. Res. Lett.* **44**, 9910–9917 (2017).
30. Murakami, H. et al. Future changes in tropical cyclone activity projected by the new high-resolution MRI-AGCM. *J. Clim.* **25**, 3237–3260 (2012).
31. Gensisi, V. A. & Mote, T. L. Downscaled estimates of late 21st century severe weather from CCSM3. *Clim. Change* **129**, 307–321 (2015).
32. Hoogewind, K. A., Baldwin, M. E. & Trapp, R. J. The impact of climate change on hazardous convective weather in the United States: Insight from high-resolution dynamical downscaling. *J. Clim.* **30**, 10081–10100 (2017).
33. Prein, A. F. et al. Simulating North American mesoscale convective systems with a convection-permitting climate model. *Clim. Dyn.* **55**, 95–110 (2020).
34. Bercos-Hickey, E., Patricola, C. M. & Gallus, W. A. Jr Anthropogenic influences on tornadic storms. *J. Clim.* **34**, 8989–9006 (2021).
35. Ashley, W. S., Haberlie, A. M. & Gensini, V. A. The future of supercells in the United States. *Bull. Am. Meteorol. Soc.* **104**, E1–E21 (2023).
36. Tochimoto, E. Environmental controls on tornadoes and tornado outbreak. *Atmos. Ocean* **60**, 399–421 (2022).
37. Rasmussen, E. N. & Blanchard, D. O. A baseline climatology of sounding-derived supercell and tornado forecast parameters. *Weather Forecast.* **13**, 1148–1164 (1998).
38. Craven, J. P. & Brooks, H. E. Baseline climatology of sounding derived parameters associated with deep, moist convection. *Natl Weather Dig.* **28**, 13–24 (2004).
39. Sakurai, K. & Kawamura, R. The environment and potential predictability of tornadoes occurred in Japan. *Tenki* **55**, 7–11 (2007).
40. Hersbach, H. et al. The ERA5 global reanalysis. *Q. J. R. Meteorol. Soc.* **146**, 1999–2049 (2020).
41. Taszarek, M. et al. Comparison of convective parameters derived from ERA5 and MERRA-2 with rawinsonde data over Europe and the United States. *J. Clim.* **34**, 3211–3237 (2021).
42. Kobayashi, S. et al. The JRA-55 reanalysis: general specifications and basic characteristics. *J. Meteorol. Soc. Jpn.* **93**, 5–48 (2015).
43. Varga, A. K. & Breuer, H. Evaluation of convective parameters derived from pressure level and native ERA5 data and different resolution WRF climate simulations over Central Europe. *Clim. Dyn.* **58**, 1569–1585 (2022).
44. Mizuta, R. et al. Over 5000 years of ensemble future climate simulations by 60 km global and 20 km regional atmospheric models. *Bull. Am. Meteorol. Soc.* **98**, 1383–1398 (2017).
45. Fujita, M. et al. Precipitation changes in a climate with 2-K surface warming from large ensemble simulations using 60-km global and 20-km regional atmospheric models. *Geophys. Res. Lett.* **46**, 435–442 (2020).
46. Sasaki, H., Murata, A., Hanafusa, M., Oh'izumi, M. & Kurihara, K. Reproducibility of present climate in a non-hydrostatic regional climate model nested within an atmosphere general circulation model. *SOLA* **7**, 173–176 (2011).

## ACKNOWLEDGEMENTS

This work is supported by the Environment Research and Technology Development Fund JPMEERF20232003 of the Environmental Restoration and Conservation Agency of Japan, the Program for the Advanced Studies of Climate Change Projection

(SENTAN) grant number JPMXD0722680734 from the Ministry of Education, Culture, Sports, Science, and Technology (MEXT), by JSPS KAKENHI grant 19H00963, and by the Research Field of Hokkaido Weather Forecast and Technology Development (endowed by Hokkaido Weather Technology Center Co. Ltd.).

## AUTHOR CONTRIBUTIONS

S.K. designed the study, prepared the figures, and wrote the manuscript. S.K., M.I., M.F., S.S., Y.O. and S.W. analyzed the d4PDF HIST and +2-K simulation results and contributed to data processing and storage. All co-authors were involved in the deliberations of this study, assisted in the writing, and approved the current version of the manuscript.

## COMPETING INTERESTS

The authors declare no competing interests.

## ADDITIONAL INFORMATION

**Supplementary information** The online version contains supplementary material available at https://doi.org/10.1038/s41612-023-00524-x.

**Correspondence** and requests for materials should be addressed to Sho Kawazoe.

**Reprints and permission information** is available at http://www.nature.com/reprints

**Publisher's note** Springer Nature remains neutral with regard to jurisdictional claims in published maps and institutional affiliations.

**Open Access** This article is licensed under a Creative Commons Attribution 4.0 International License, which permits use, sharing, adaptation, distribution and reproduction in any medium or format, as long as you give appropriate credit to the original author(s) and the source, provide a link to the Creative Commons license, and indicate if changes were made. The images or other third party material in this article are included in the article's Creative Commons license, unless indicated otherwise in a credit line to the material. If material is not included in the article's Creative Commons license and your intended use is not permitted by statutory regulation or exceeds the permitted use, you will need to obtain permission directly from the copyright holder. To view a copy of this license, visit http://creativecommons.org/licenses/by/4.0/.

© The Author(s) 2023